Technical Report

Heliborne Magnetic, Spectrometric and TDEM Survey

Hemlo Project, Marathon area
Thunder Bay District, Ontario
2016

North American Exploration Ltd.
68 Westbrook Dr., RR#5
Komoka, ON, Canada, N0L 1R0

Prospectair Geosurveys

Dynamic Discovery Geoscience

Prepared by:
Joël Dubé, P.Eng.

August 2016

Dynamic Discovery Geoscience
7977 Décarie Drive
Ottawa, ON, K1C 3K3
jdube@ddgeoscience.ca
819.598.8486

Survey flown by :

15 chemin de l'Étang
Gatineau, Québec J9J 3S9
(819)661-2029
Fax: 1.866.605.3653
contact@prospectair.ca

Table of Contents

FIGURES

TABLES

I. INTRODUCTION

PROSPECTAIR conducted a heliborne magnetic (MAG), spectrometric (SPEC) and time-domain electromagnetic (TDEM) survey for the mineral exploration company North American Exploration Ltd. on its Hemlo Project, located within the Wabikoba Lake area (G-0620), Thunder Bay Mining Division, and overlapping NTS Mapsheets 042C12 and 042C13, Province of Ontario (Figures 1 and 2). The survey was flown on August 21st and 22nd, 2016.

Figure 1: **General survey location**

One survey block was flown for a total of 430 l-km. A total of 2 production flights were performed using PROSPECTAIR's Eurocopter EC120B, registration C-GEDI. The helicopter and survey crew operated out of the Marathon Airport located approximately 33 km west of the block (Figure 2).

Table 1: **Survey block particulars**

Block	NTS Mapsheet	Line-km flown	Flight number	Date Flown
Hemlo	042C12 and 042C13	430 l-km	Flt 1 and 2	August 21st and 22nd

Figure 2: **Survey Location and base of operation**

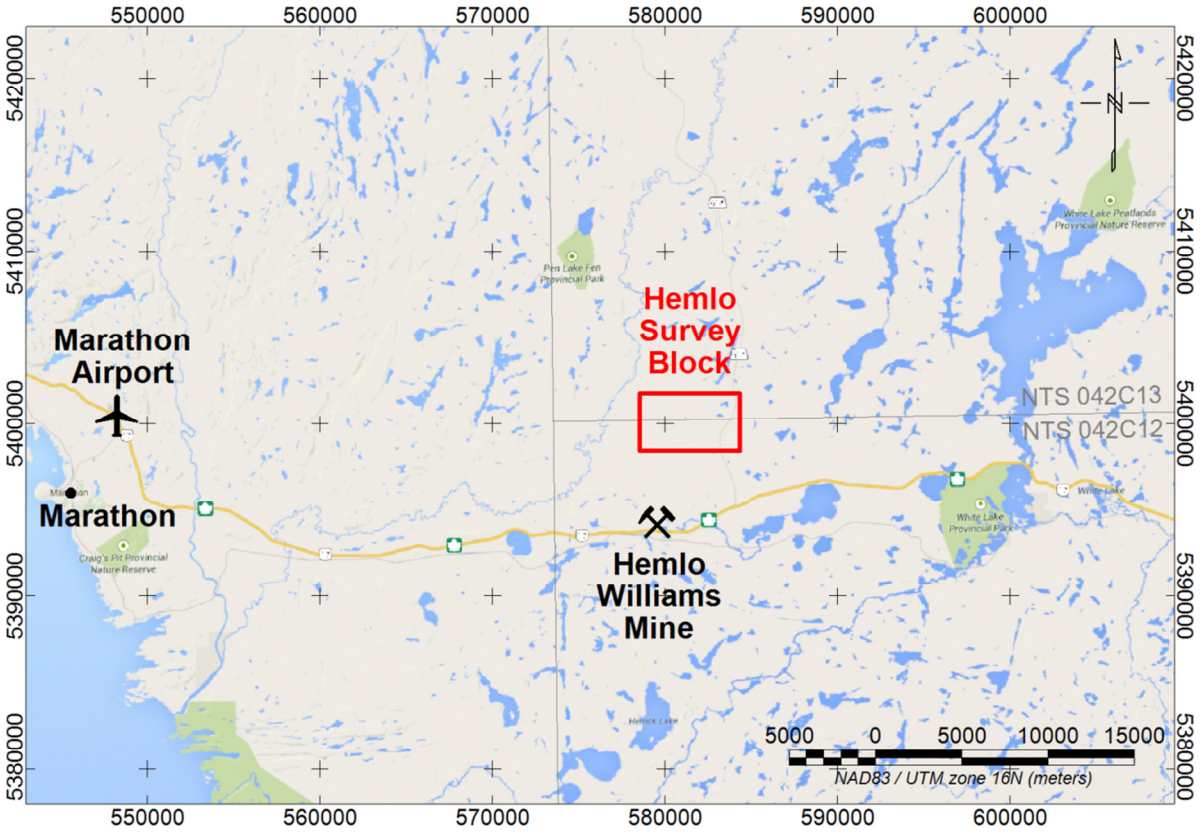

The Hemlo block was flown with traverse lines at 50 m spacing and control lines spaced every 500 m. The survey lines were oriented N000. The control lines were oriented perpendicular to traverse lines. The nominal survey height for the MAG-SPEC-TDEM survey was set to 85 m, but the active topography and a power line found in the area resulted in an average height above ground of the helicopter of 87 m, with the mag sensor and receiver coil at 62 m, and the transmitter loop at 37 m above the ground. The average survey flying speed (calculated equivalent ground speed) was 30.7 m/s. The survey area is covered by forest with a few lakes and wetlands, and the topography is characterized by gentle hills, which are fairly typical characteristics of the area east of Marathon. The elevation is ranging from 240 to 384 m above mean sea level (MSL). The southern limit of the Hemlo Property is located only 4 km north of the producing Hemlo Williams Mine. Coordinates outlining the survey block are given in Table 2, with respect to NAD-83 datum, UTM projection zone 16N. The survey covered the mining claims shown on Figure 3 and listed in Table 3.

Table 2: **Hemlo survey outline**

Easting	Northing
578540	5398430
584320	5398430
584320	5401780
578540	5401780

Table 3: **Hemlo Mineral claims**

Claim No	Claim Units	Area	NTS Map Sheet
TB 4267354	8	Wabikoba Lake Area	042C12 & 042C13
TB 4267355	16	Wabikoba Lake Area	042C12 & 042C13
TB 4267356	16	Wabikoba Lake Area	042C12
TB 4267357	16	Wabikoba Lake Area	042C12 & 042C13
TB 4267358	14	Wabikoba Lake Area	042C12
TB 4267359	16	Wabikoba Lake Area	042C12 & 042C13
TB 4267360	14	Wabikoba Lake Area	042C12

Figure 3: **Hemlo survey lines and mineral claims**

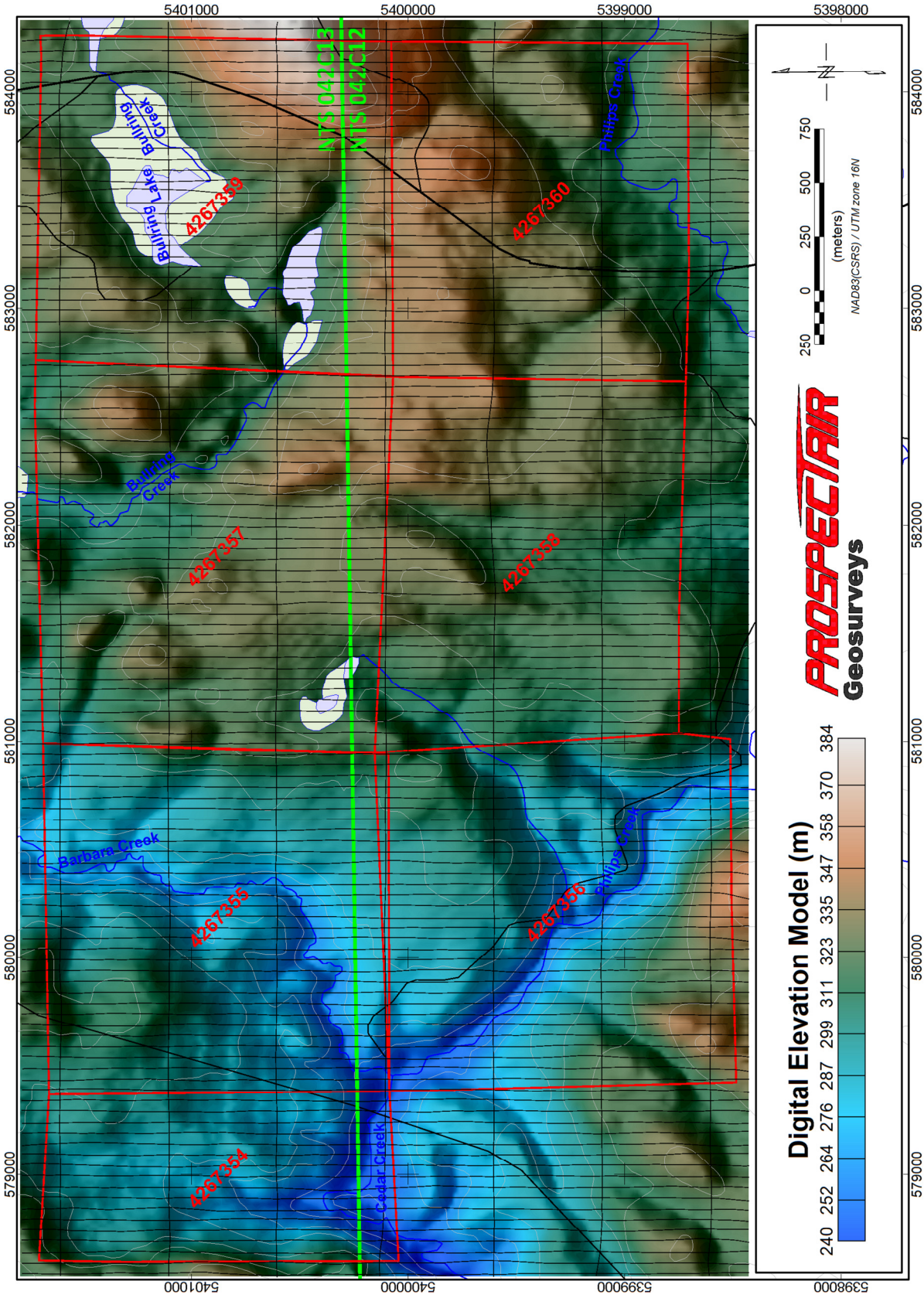

II. SURVEY EQUIPMENT

PROSPECTAIR provided the following instrumentation for this survey:

Airborne Magnetometers
Geometrics G-822A
Both the ground and heliborne systems used a non-oriented (strap-down) optically-pumped Cesium split-beam sensor. These magnetometers have a sensitivity of 0.005 nT and a range of 15,000 to 100,000 nT with a sensor noise of less than 0.02 nT. The heliborne sensor was mounted in a bird made of non-magnetic material located 25 m below the helicopter when flying. Total magnetic field measurements were recorded at 10 Hz in the aircraft. The ground system was recording magnetic data at 1 sample every second.

Time-Domain Electromagnetic Transmitter and Receiver
ProspecTEM I
Prospectair Geosurveys significantly modified and improved the *Emosquito II* that was built by THEM Geophysics of Gatineau (Québec) to develop ProspecTEM. It is a powerful light-weight system adapted for small size helicopters and easy manoeuvrability enabling the system to be flown as close to the ground as safely possible and ensuring maximum data resolution. Advanced signal processing technique and a full processing package was developed in house to optimize the ProspecTEM data. The technical specifications are listed below in Table 4.

ProspecTEM system employs a transient or time-domain electromagnetic transmitter that drives an alternating current through an insulated electrical coil system. The towing bridle is constructed from a Kevlar rope and multi-paired shielded cables. It is attached to the helicopter by a weak link assembly. An onboard harness with outboard connectors mounted on a plate allows for quick disconnection or connection of the exterior elements. The system uses a 4 KW generator and a large condenser to transmit alternating 2.75-ms half sine pulses with intervening off-times of 13.916 ms electric pulse, 60 pulses per second.

The current in the coil produces an electromagnetic field. Termination of the current flow is not instantaneous, but occurs over a very brief period of time (a few microseconds) known as the ramp time, during which the magnetic field is time-variant. The time-variant nature of the primary electromagnetic field, which propagates downward and outward into the subsurface, induces eddy currents which characteristics are governed by rocks conductivity distribution. These eddy currents generate a secondary electromagnetic field, in accordance with Faraday's Law. This secondary field immediately begins to decay in the process. Measurements of the secondary field are made only during the time-off period by a vertical component receiver located almost half way between the helicopter and the transmitter loop. It is placed with the magnetometer taped to a horizontal boom which supports the receiving coils tear-drop shape vessel at its end. The boom has an elastic suspension. A proprietary suspension system protects the orthogonal coils assembly and

limits the total field excursions. The tear-drop vessel acts as a vane and maintains the mast in the line of flight.

Depth of investigation depends on the time interval after shutoff of the current, since at later times the receiver is sensing eddy currents at progressively greater depths. The intensity of the eddy currents at specific times and depths is determined by the bulk conductivity of subsurface rock units and their contained fluids.

Table 4: **Technical specifications of the ProspecTEM Time-Domain system**

Item	Specification
Transmitter:	
Loop Diameter:	5.6 meters
Current Waveform:	Half-Sine
Turns:	2
Pulse Length	2.75 ms
Frequency	30 Hz
Loop Area	25 m²
Peak Current	3000A
Tow Cable Length	65 meters
Self-Powered	13HP Honda coupled with 28 Volts Alternator
Receiver:	
Coils axis	Z
Configuration	Coaxial (Z)
Two channels	Current and Z
Max Sampling rate	1000 points per half cycle at 90 Hz
Survey sampling rate	1000 per half cycle at 30Hz
Sampling	Full waveform
Gates	Programmable
On time signal	Recorded
Mechanical:	
Maximum survey speed:	120 km per hour
Transmitter height	30 meters AGL
Receiver height	60 meters
Weight (Total)	200 kg

Figure 4: **ProspecTEM system configuration**

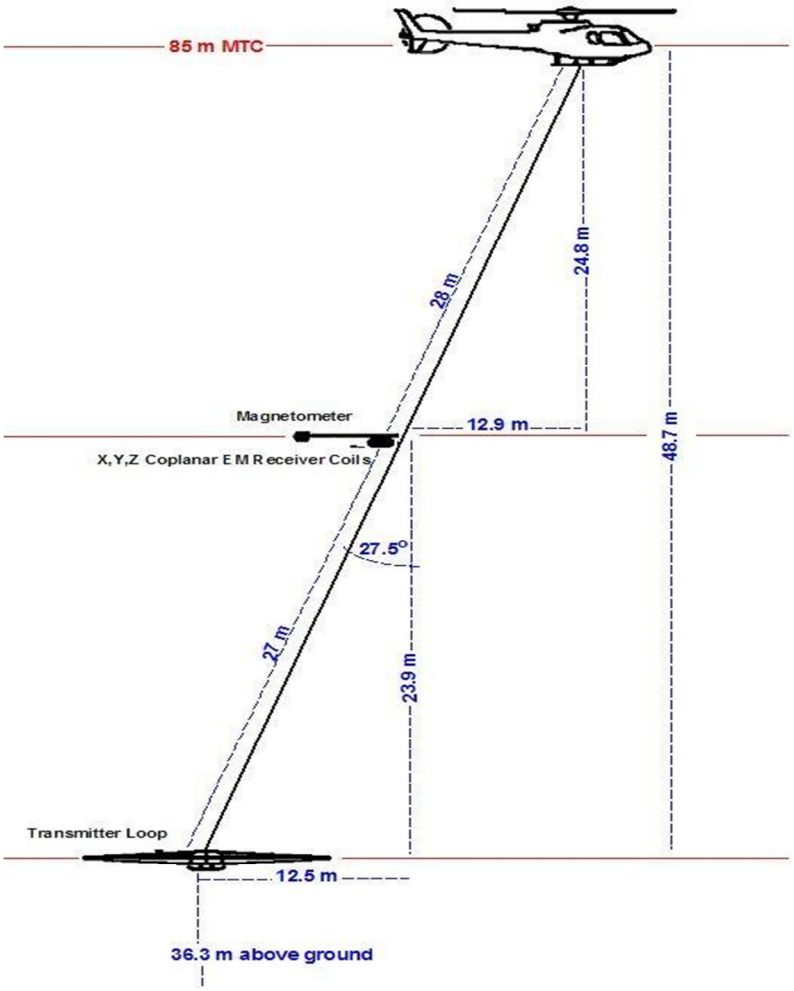

Real-Time Differential GPS

Omnistar DGPS

PROSPECTAIR uses an OmniStar differential GPS navigation system to provide real-time guidance for the pilot and to position data to an absolute accuracy of better than 5 m. The *Omnistar* receiver provides real-time differential GPS for the Agis on-board navigation system. The differential data set was relayed to the helicopter via the Omnistar network appropriate geosynchronous satellite for the survey location. The receiver optimizes the corrections for the current location.

Airborne Navigation and Data Acquisition System

Pico-Envirotec AGIS-XP system

The Airborne Geophysical Information System (AGIS-XP) is advanced, software driven instrument specifically designed for mobile aerial or ground geophysical survey work. The AGIS instrumentation package includes an advanced Satellite navigation (GPS), real-time flight path information that is displayed over a map image (BMP format) of the area, and reliable data acquisition software. Thanks to simple interfacing, the radar and barometric altimeters, the TDEM system and the Geometrics magnetometer are easily integrated into the system and digitally recorded. Automatic synchronization to the GPS position and time provides very close correlation between data and geographical position. The AGIS is equipped with a software suite allowing easy maintenance, upgrades, data QC, and project and survey area layout planning.

Gamma Ray Spectrometer System

Radiation Solutions RSX-5 Spectrometer and detector package

PROSPECTAIR mounted a 16 liters (4 crystals) downward-looking crystal and 4 liters (1 crystal) upward-looking crystal, and analyze gamma radiation with a Radiation Solutions Inc. RSX-5 256-channel spectrometer. The RSX-5 is self-calibrating and has automatic gain control, which eliminates the use of radioactive sources in the field. The spectrometer records total count, counts for potassium, uranium and thorium, along with the entire 256 channels spectra and live-time at a rate of 1 Hz.

Magnetic Base Station

GEM GSM-19

A GEM GSM-19 Overhauser magnetometer, a computer workstation and a complement of spare parts and test equipment serve as the base station. PROSPECTAIR establish the base station in a secure location with low magnetic noise. The GSM-19 magnetometer has resolution of 0.01 nT, and 0.2 nT accuracy over its operating range of 20,000- to 100,000 nT. The ground system was recording magnetic data at 1 Hz.

Altimeters

Free Flight Radar Altimeter

The Free Flight radar altimeter measures height above ground to a resolution of 0.5 m and an accuracy of 5% over a range up to 2,500 ft. The radar altimeter data is recorded and sampled at 10 Hz.

Prospectair Digital Barometric Pressure Sensor

The barometric pressure sensor measures static pressure to an accuracy of ± 4 m and resolution of 2 m over a range up to 30,000 ft above sea level. The barometric altimeter data are sampled at 10 Hz.

Survey helicopter

Eurocopter EC120B (registration C-GEDI)

The survey was flown using Prospectair's EC120B helicopter that handles efficiently the equipment load and the required survey range. Table 5 lists the EC120B technical specifications and capacity, and the aircraft is shown in Figure 5.

Table 5: **Technical specifications of the EC120B Eurocopter helicopter**

Item	Specification
Powerplant	One 376kW (504hp) Turbomeca Arrius 2F
Rate of climb	1,150 ft/min
Cruise speed	223 km/h – 120 kts
Service ceiling	17,000 ft
Range with no reserve	710 km
Empty weight	991 kg
Maximum takeoff weight	1,715 kg

Figure 5: **Eurocopter EC120B**

III. SURVEY SPECIFICATIONS

Data Recording

The following parameters were recorded during the course of the survey:

In the helicopter:

- GPS positional data (time, latitude, longitude, altitude, heading and accuracy (PDOP)) recorded at intervals of 0.1 s;
- Total magnetic field recorded at intervals of 0.1 s;
- Airborne spectrometer data recorded at intervals of 0.1 s;
- Pressure as measured by the barometric altimeter at intervals of 0.1 s;
- Outside air temperature recorded by the pilot every flight;
- Terrain clearance as measured by the radar altimeter at intervals of 0.1 s;
- Z and Current TDEM channels at 90000Hz;
- Potassium, Uranium, Thorium and total counts at intervals of 1 s;
- 256 channels gamma-ray spectra for downward and upward crystals at 1Hz.

At the base and remote magnetic ground stations:

- Total magnetic field: recorded at intervals of 1 s;
- GPS time recorded every 1s to synchronize with airborne data;
- Potassium, Uranium, Thorium and total counts monitored pre and post flights.

Technical Specifications

The data quality control was performed on a daily basis. The following technical specifications were adhered to:

- *Height* – 85m target terrain clearance for the survey except in areas where Transport Canada regulations prevent flying at this height, or as deemed necessary by the pilot to ensure safety. The altitude tolerances are limited to no more than 30 m difference between traverse lines and control lines.
- *Airborne Magnetometer Data* - The noise envelope not to be exceeded 0.5 nT more than 500 m line-length without a reflight.
- *Diurnal Specifications* – A maximum tolerance of 5.0 nT (peak to peak) deviation from a long chord of one minute at the base station.
- *Precipitation Limitations* – Varying ground moisture conditions affect the airborne radioactivity measurements. No survey flying should be undertaken during or for 3 hours after measurable precipitation. In the event of heavy precipitation yielding more than 2 cm of ground soaking rain, flying should be suspended for at least 12 hours after end of precipitation.
- *EM data* – No spikes on Z channel and constant current.
- *Flying Speed* – The average ground speed for the survey aircraft should be 120 kph. The acceptable high limit is 160 kph over flat topography.
- *Radar Altimeter* – minimal accuracy of 5%, minimum range of 0-2500 m.
- *Barometer* – Absolute air pressure to 0.1 kPa.
- *Flight Path Following*
  Traverse lines: Azimuth N000, 50 m spacing.
  Control Lines: Azimuth N090, 500 m spacing.

IV. SYSTEM TESTS

Magnetometer System Calibration

The survey configuration using a bird towed 25 m below any magnetic piece of the helicopter allows the simplification of the magnetic calibration requirement. Consequently, heading error and aircraft movement noise was considered negligible and no correction was applied to the data.

Instrumentation Lag

The data lag is a combination of two factors: 1) the time difference between when a reading is sensed, and when that value is recorded by the acquisition system, and 2) the time taken for the sensor to arrive at the location of the GPS antenna. The second factor is defined by the physical distance between the GPS antenna and any given sensor, and the speed of the aircraft. The total magnetic lag value for the AGIS acquisition system has been calculated to be 2.15 s. Figure 6 shows a graph of the lag corrected magnetic data compared to raw data over a significant magnetite anomaly. The TDEM and SPEC lag was calculated to be 0.35 s.

Figure 6: **Comparison between lag corrected and raw magnetic data**

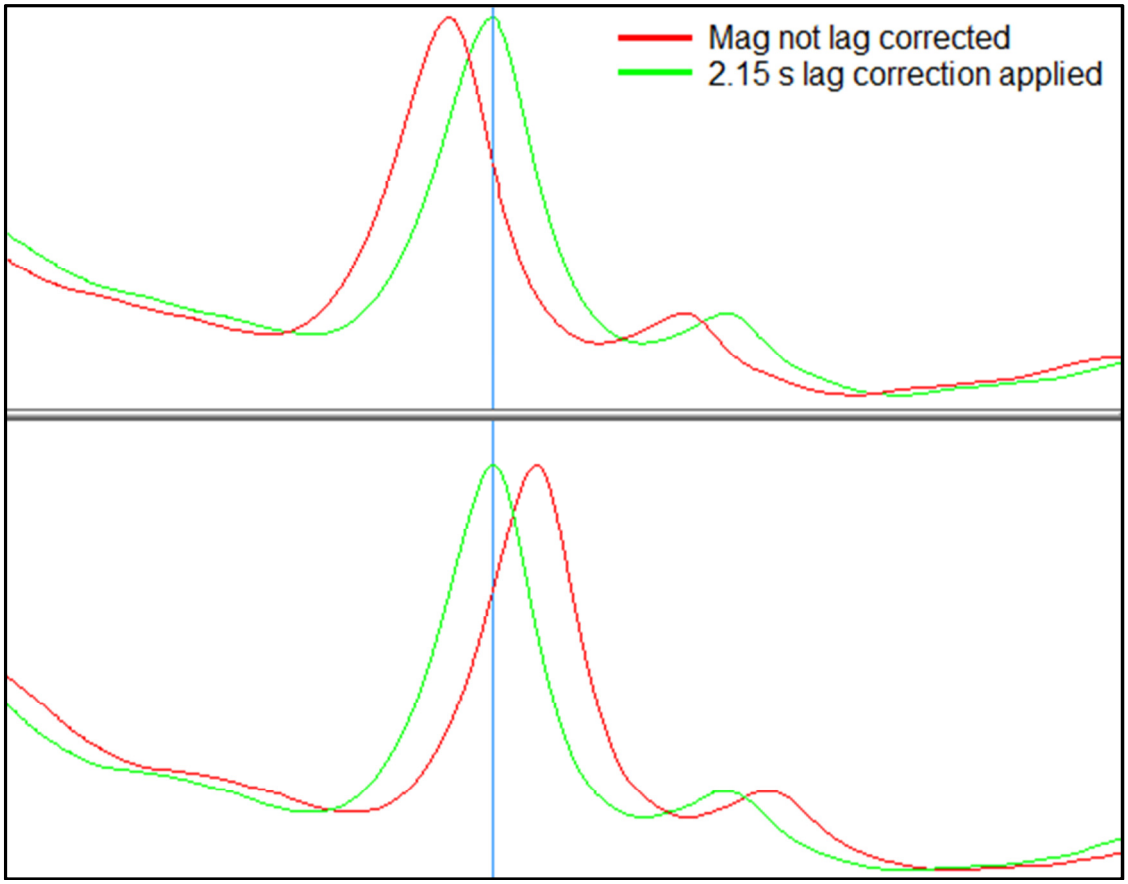

Stripping Ratios

The stripping ratios for the gamma-ray spectrometer were determined by the RSX-5 manufacturer, Radiation Solution Inc, at their Mississauga facility on May 26th, 2016. Each detector was tested separately and the test results were averaged to create stripping ratios for this system. See Table 6 for a list of stripping ratios.

Table 6: **Stripping Ratios**

STRIPPING RATIOS	
Thorium into Uranium (Alpha)	0.268
Thorium into Potassium (Beta)	0.415
Uranium into Potassium (Gamma)	0.759
Uranium into Thorium (A)	0.043
Potassium into Thorium (B)	-0.001
Potassium into Uranium (G)	-0.001

Attenuation Coefficients

The exponential height attenuation coefficients for the spectrometer were calculated using the data acquired during a post-survey test flight over the GSC test range at Breckenridge, Québec, on August 18th, 2013. The calibration flights were carried out from approximately 50 m to 260 m mean terrain clearance at 30 m intervals. A series of background measurements were made at the same altitudes over the Ottawa River to determine the background due to cosmic radiation, radon decay products in the air and the radioactivity of the aircraft and equipment. Results of this test are given in Table 7.

Table 7: **Spectrometer Calibration Test Data**

SPECTROMETER CALIBRATION TEST DATA				
Altitude at STP (m)	Total counts (cps)	Potassium (cps)	Uranium (cps)	Thorium (cps)
48.4	1054.5	118.0	8.9	26.8
72.1	883.6	92.9	7.0	23.4
99.1	722.8	73.0	5.4	18.6
128.0	591.4	55.9	5.2	15.7
156.9	483.1	42.9	3.8	12.7
183.3	401.5	32.9	3.2	10.6
215.9	322.6	25.9	2.4	8.9
238.6	277.0	22.5	1.9	7.6

After correction for background and stripping, the variation in count rate with effective height was used to determine the attenuation coefficients shown in Table 8.

Table 8: **Attenuation Coefficients**

ATTENUATION COEFFICIENTS	
Total	-0.0071
Potassium	-0.0089
Uranium	-0.0085
Thorium	-0.0068

Spectrometer System Sensitivity

A pre-survey test flight was carried out over the GSC test range at Breckenridge, Québec on August 18th, 2013. The test flight served to determine system sensitivities through comparison of airborne data with data acquired on the ground, as well as to determine the variation of the window counts with aircraft altitude (attenuation coefficients, see above).

The ground measurements were made with a Radiation Solution RS-125 portable gamma ray spectrometer and acquired at 32 different sites along the 10 km length of the calibration range. Measurements were also made with the portable spectrometer on the Ottawa River to determine background radiation due to cosmic radiation, radon decay products in the air and any radioactivity of the equipment. The background was subtracted from the ground measurements and the ground concentrations of potassium, uranium and thorium were determined by calibration of the portable spectrometer performed at Radiation Solution facilities in Mississauga, Ontario.

The sensitivities of the airborne system to potassium, equivalent uranium, and equivalent thorium were calculated by dividing the average count rates corrected to an effective height of 45 m above ground by the ground concentrations of the test range. Results are presented in Table 9.

Table 9: **System Sensitivities from Breckenridge Test**

SYSTEM SENSITIVITIES - Breckenridge			
	Average counts at 45 m	Ground Concentrations	Sensitivities
Potassium	121.843 cps	2.116 %	57.592 cps/%
Equivalent Uranium	9.162 cps	1.022 ppm	8.966 cps/ppm
Equivalent Thorium	27.531 cps	9.463 ppm	2.910 cps/ppm

Cosmic and Aircraft Background

For the EC120B helicopter, a cosmic and aircraft background test was performed on August 5th, 2013, over the St-Lawrence River. The test flights consisted of flying at heights of 1000 m to 3000 m above ground level at 300 m intervals, recording data for 8 to 10 minutes at each level. Coefficients are determined by linear regression of cosmic counts versus each spectral window as described in the IAEA Report 323 (1991). Table 10 lists the computed cosmic and aircraft background coefficients.

Table 10: **EC120B Cosmic Coefficients**

COSMIC COEFFICIENTS		
	Cosmic Coefficient	**Aircraft Background**
Total	1.1219	58.269
Potassium	0.0647	10.902
Uranium	0.0570	0.860
Thorium	0.0684	-0.829
Upward	0.0120	0.743

Radon Corrections and Ground Component Coefficients

Radon background would normally be monitored through the use of upward looking detectors. However, given that the block was surveyed over the course of only two days, it was not possible to relate the count rate in the uranium window from the upward detectors to the count rate in the potassium, uranium, thorium and total count windows from the downward facing detectors by using several over-water test lines. As a result, neither radon correction coefficients nor ground component coefficients were calculated for this survey.

V. FIELD OPERATIONS

The survey operations were conducted out of the Marathon Airport on August 21st and 22nd 2016. The MAG-SPEC-TDEM data acquisition required 2 flights. At the end of each production day, the data were sent to the DD Geoscience office via internet. The data were then checked for Quality Control to ensure they fulfilled contractual specifications. The full dataset was inspected prior to provide authorization for the field crew to demobilize. The GEM-19 magnetic base station was set up in a magnetically quiet area near Hemlo, in between the railway and highway 17, at latitude 48.6881740°N, longitude 85.9799183°W. The survey pilot was Alain Tremblay and the survey system technician was Jonathan Drolet.

Figure 7: **Example of a magnetic base station setup**

VI. DIGITAL DATA COMPILATION

Data compilation including editing and filtering, quality control, and final data processing was performed by Joël Dubé, P. Eng. Processing was performed on high performance desktop computers optimized for quick daily QC and processing tasks. Geosoft software Oasis Montaj version 8.5.5 and Matlab 7 R2009B were used.

Magnetometer Data

The airborne magnetometer data, recorded at 10 Hz, were plotted and checked for spikes and noise on a flight basis. A 2.15 second lag correction was applied to all data to correct for the time delay between detection and recording of the airborne data.

Ground magnetometer data were recorded at 1 sample every second and interpolated by a spline function to 10 Hz to match airborne data. Data were inspected for cultural interference and edited where necessary. Some low-pass filtering was deemed necessary on the ground station magnetometer data to remove minor high frequency noise. The diurnal variations were removed by subtracting the ground magnetometer data to the airborne data and by adding back the average of the ground magnetometer value.

Levelling corrections were performed using intersection statistics from traverse and tie lines. After statistical levelling was considered satisfactory, decorrugation was applied on the data to remove any remaining subtle non-geological features oriented in the direction of the traverse lines.

Once the Total Magnetic Intensity (TMI) was gridded, its First Vertical Derivative (FVD) and Second Vertical Derivative (SVD) were calculated to enhance narrower geological features. Finally, the component of the normal Earth's magnetic field, described by the International Geomagnetic Reference Field (IGRF), has been removed from the TMI to yield the residual TMI. This ensures that the very long wavelength signal within the block is indeed originating from the geology.

Radar Altimeter Data

The terrain clearance measured by the radar altimeter in metres was recorded at 10 Hz. The data were filtered to remove high frequency noise using a 1 sec low pass filter. The final data were plotted and inspected for quality.

Positional Data

Real time DGPS correction provided by Omnistar was applied to the recorded GPS positional data. No post-flight DGPS processing was made using a GPS base station.

Positional data (Lat, long, UTM X, UTM Y, geoid height) were recorded at 10 Hz sampling rate and all data processing was performed in the WGS-84 datum. The delivered data were provided in X, Y locations in UTM projection zone 15 North, with respect to the NAD-83 datum. Altitude data were initially recorded relative to the GRS-80 ellipsoid, but are delivered as orthometric heights (MSL elevation).

Radiometric Data

The AGIS acquisition system is sampling the RSI spectrometer every 0.1 sec to make a constant 10 Hz recording synchronized with magnetic data and other survey equipment.

Standard Corrections

Spectrometer data were corrected as documented in the Geological Survey of Canada Open File No. 109 and the IAEA report "Airborne gamma-ray spectrometer surveying; Technical Report Series No. 323 (International Atomic Energy Agency, Vienna).

The gamma-ray spectrometry processing parameters are summarized in Table 11.

Table 11: **Spectrometer Data Processing Parameters**

Spectrometer Processing Parameters		
WINDOW	COSMIC STRIPPING (B)	BACKGROUND (A)
Total	1.1219	58.269
Potassium	0.0647	10.902
Uranium	0.0570	0.860
Thorium	0.0684	-0.829
Upward	0.0120	0.743
RADON COMPONENT	A	B
Total (I_r)	N/A	N/A
Potassium (K_r)	N/A	N/A
Thorium (T_r)	N/A	N/A
UP (u_r)	N/A	N/A
GROUND COMPONENT	A1	A2
UP (u_g)	N/A	N/A
STRIPPING RATIOS		INCREASE IN HEIGHT (per metre)
alpha	0.268	0.00049
beta	0.415	0.00065
gamma	0.759	0.00069
a	0.043	
b	-0.001	
g	-0.001	
ATTENUATION COEFFICIENTS		
Total	-0.0071	
Potassium	-0.0089	
Uranium	-0.0085	
Thorium	-0.0068	
SENSITIVITIES		
Potassium	57.592 cps/%	
Uranium	8.966 cps/ppm	
Thorium	2.910 cps/ppm	

Before gridding, the following corrections are applied to the spectrometer data in the order shown:

1) Dead time correction

The system live time is recorded by the spectrometer and represents the time that the system was available to accept incoming gamma radiation pulses. Live time is reduced, and dead time increased, as count rates increase and the time taken by the spectrometer to process measured pulses increases. The recorded live time per second in the RSX-5 spectrometer corresponds to a constant value of 0.999sec. The dead time is considered marginal compared to older spectrometer due to new circuitry and technology in the RSI package. The dead-time correction is applied to each window in both the upward and downward looking detector data using the following equation: N = n / t

where: N = the corrected count rate in each channel
n = the raw count recorded in each second
t = the recorded live time (fraction of a second).

2) Calculation of effective height above ground level (AGL)

A 1 sec low pass filter is applied to 10Hz radar altimeter data, and a 5 sec low pass filter is applied to 10Hz barometric pressure. The barometric data are then used with the manually recorded temperature to convert the radar altimeter data to effective height at standard pressure and temperature (STP) as follows:

$$h_e = h \times \frac{273.15}{T + 273.15} \times \frac{P}{1013.25}$$

where: h_e = the effective height
h = the observed radar altitude in metres
T = the observed air temperature in degrees Centigrade, and
P = the observed barometric pressure in millibars.

3) Height adaptive filter

By convention, data collected at a terrain clearance greater than 200 m are considered less reliable due to the low count rates received by 4 downward crystals and consequent low signal to noise ratio. Height adaptive filtering, which consists in increasing filtering as a function of clearance, can then be applied to further reduce the noise at these heights. The maximum terrain clearance for this project only slightly exceeded 130m based on the calculated effective height. Consequently, no height adaptive filtering was required.

4) Removal of cosmic radiation and aircraft background radiation

A low pass filter with a limit of 10 sec wavelength is applied to 10Hz Cosmic data to reduce statistical noise. Cosmic radiation and aircraft background radiation are removed from each spectral window using the cosmic coefficients and aircraft background values determined from test flight data using the following the equation:

$$N = a + bC$$

where: N = the combined cosmic and aircraft background in each spectral window,
a = the aircraft background in the window,
b = the cosmic stripping factor for the window, and
C = the cosmic channel count.

5) Radon background corrections

A 30 sec non-linear filter is applied to 10 Hz downward uranium, downward thorium and upward uranium count data for the purposes of the radon correction only. The upward uranium count channel is then filtered with a 5 sec low pass filter to smooth it further before the radon correction. The radon component in the uranium window is calculated using the radon coefficients determined from the survey data using the following equation:

$$U_r = \frac{u - a_1 U - a_2 T + a_2 b_T - b_u}{a_u - a_1 - a_2 a_T}$$

where: U_r = the radon background measured in the downward uranium window,
u = the filtered observed count in the upward uranium window,
U = the filtered observed count in the downward uranium window,
T = the filtered observed count in the downward thorium window,
a_1 and a_2 = the ground coefficients,
a_u and b_u = the radon coefficients for uranium,
a_T and b_T = the radon coefficients for thorium.

The radon counts in the total count, potassium and thorium downward windows are then calculated from U_r using the following equations:

$$u_r = a_u U_r + b_u$$
$$K_r = a_K U_r + b_K$$
$$T_r = a_T U_r + b_T$$
$$I_r = a_I U_r + b_I$$

Where Ur is the radon component in the upward uranium window, Kr, Ur, Tr and Ir are the radon components in the various windows of the downward detectors, and a and b are the radon calibration coefficients.

Note that the radon correction wasn't applied on the final data. It was deemed unnecessary considering the very low influence of radon on survey lines and the low counts in the upward crystal related to radon gas. The application of radon correction determined by the upward detector methodology described above was inducing undesirable noise without adding any benefit to the data quality.

6) Stripping

The stripping ratios for the spectrometer system are determined experimentally. The stripped count rates for the potassium, uranium and thorium downward windows are calculated using the following equations:

$$N_K = \frac{n_{Th}(\alpha\gamma - \beta) + n_U(\alpha\beta - \gamma) + n_K(1 - a\alpha)}{A}$$

where A has the value:

$$A = 1 - g\gamma - a(\gamma - gb) - b(\beta - \alpha\gamma)$$

$$N_{Th} = \frac{n_{Th}(1 - g\gamma) + n_U(b\gamma - a) + n_K(ag - b)}{A}$$

$$N_U = \frac{n_{Th}(g\beta - \alpha) + n_U(1 - b\beta) + n_K(b\alpha - g)}{A}$$

and where

n_K, n_U and n_{Th} = the unstripped potassium, uranium and thorium downward windows counts,

N_K, N_U and N_{Th} = the stripped potassium, uranium and thorium downward windows counts,

α, β, and γ = the forward stripping ratios, and

a, b and g = the reverse stripping ratios.

α, β, and γ are adjusted for effective height (as calculated above) by standard factors given in Table 11.

7) Altitude attenuation correction

This correction normalizes the data to a constant terrain clearance of 45m above ground level (AGL) at standard temperature and pressure (STP). Attenuation coefficients for each of the downward windows were determined from test flights. The measured count rate is related to the actual count rate at the nominal survey altitude by the equation:

$$N_s = N_m(e^{\mu(h_o - h)})$$

where: N_s = the count rate normalized to the nominal survey altitude, h_o,
N = the background corrected, stripped count rate at effective height h,
μ = the attenuation coefficient for that window,
h_o = the nominal survey altitude, and
h = the effective height.

The effective height was determined in step 2.

8) Conversion to radio element concentration

Sensitivities are determined experimentally from the test flight data. The units of the count rates in each spectral window are converted to "Apparent Radio Element Concentrations" using the following equation:

$$C = N / S$$

where: C = the concentration of the element(s)
N = the window counts after dead time, background, stripping and attenuation correction
S = the broad source sensitivity for the window.

Potassium concentration is expressed as a percentage and equivalent uranium and thorium as parts per million of the accepted standards. Uranium and thorium are described as "equivalent" since their presence is inferred from gamma-ray radiation from daughter elements (^{214}Bi for uranium, ^{208}Tl for thorium).

TDEM Data

The PicoEnvirotec EM Digital Acquisition System records the vertical component (Z) of the receiver coils at a sampling rate of 90000Hz. There is 30 full cycles (60 half cycles) of the full waveform (Tx ON and OFF time) every second.

The first data manipulation involves a stacking procedure where each half cycle is weighted with respect to the previous cycle (±¼), the next cycle (±¼) and its own value (± ½). The positive and negative signs of the respective multiplication coefficients are used to make positive all negative half cycles. The next step is the half cycle averaging corresponding to the desired sampling rate. In the present case, from the 60 stacked positive half cycles per second, 6 consecutive half cycles are averaged to produce one sample every 0.1 sec.

The windowing settings for the 40 different channels are presented in Table 12. Channels 1 to 11 correspond to the ON-time measurements and channels 12 to 40 correspond to the OFF-time. Channel 12 isn't used for interpretation and mapping as it exists some 'ramp-off' effect that alters the data quality. Each window is filtered with a median filter removing spikes and with a finite impulse response (FIR) selective filter of the 251th order improving the signal to noise ratio. A lag correction of 0.35 sec was applied to the data after being empirically determined by flying a sharp anomaly in two opposite direction.

Table 12: **Setting used in the windowing of the full waveform**

Channel #	Starting time (msec)	Width (msec)	Pulse	Channel #	Starting time (msec)	Width (msec)	Pulse
1	0.16667	0.01667	**ON**	**21**	3.15000	0.53333	**OFF**
2	0.25000	0.01667	**ON**	**22**	3.26667	0.53333	**OFF**
3	0.33333	0.01667	**ON**	**23**	3.40000	0.53333	**OFF**
4	1.30000	0.01667	**ON**	**24**	3.40000	1.10000	**OFF**
5	1.31667	0.01667	**ON**	**25**	3.45000	1.10000	**OFF**
6	1.33333	0.01667	**ON**	**26**	3.65000	1.10000	**OFF**
7	2.58333	0.01667	**ON**	**27**	3.88333	1.10000	**OFF**
8	2.66667	0.01667	**ON**	**28**	4.13333	1.10000	**OFF**
9	2.80000	0.08333	**ON**	**29**	4.43333	1.10000	**OFF**
10	2.81667	0.08333	**ON**	**30**	4.76667	1.10000	**OFF**
11	2.83333	0.08333	**ON**	**31**	5.16667	1.10000	**OFF**
12	2.85000	0.16667	**RAMP**	**32**	5.20000	2.20000	**OFF**
13	2.86667	0.18333	**OFF**	**33**	5.55000	2.20000	**OFF**
14	2.86667	0.25000	**OFF**	**34**	6.13333	2.20000	**OFF**
15	2.86667	0.36667	**OFF**	**35**	6.78333	2.20000	**OFF**
16	2.91667	0.36667	**OFF**	**36**	7.51667	2.20000	**OFF**
17	2.91667	0.53333	**OFF**	**37**	8.36667	2.20000	**OFF**
18	2.95000	0.53333	**OFF**	**38**	9.33333	2.20000	**OFF**
19	3.00000	0.53333	**OFF**	**39**	10.4500	2.20000	**OFF**
20	3.03333	0.53333	**OFF**	**40**	11.7000	2.20000	**OFF**

As for the magnetic data, levelling corrections were applied to the TDEM data using intersection statistics from traverse and tie lines, as well as light decorrugation based on gridded information, in order to remove base line offsets. Both the non-levelled and levelled TDEM data are delivered in the project's databases.

Gridding

The magnetic, radiometric and TDEM data were interpolated onto regular grids using minimum curvature and bi-directional gridding algorithms to create two-dimensional grids equally incremented in x and y directions.

The final grids were created with 10 m grid cell size, appropriate for the survey lines spaced at 50 m. Traverse lines were used in the gridding process.

VII. RESULTS AND DISCUSSION

General

The following discussion presents the helicopter-borne MAG, SPEC and TDEM data as well as a basic interpretation, which is solely based on the data acquired in this project. Further interpretation work should include other geoscientific information, but is beyond the scope of this report.

Since the surveyed area borders the Hemlo Gold Deposit (HGD), a brief review of the geophysical literature has been performed, and is summarized here. The deposit itself does not respond to any EM methods (Pemberton and al. 1984), as the gold mineralization is associated to disseminated molybdenite and pyrite, which are not abundant enough to generate EM conductors, but enough to respond very well to the ground IP/resistivity technique (Hallof et al., 1984). Magnetic data has been used with success to help mapping the geology, stratigraphy and structures controlling the mineralization. In the case of the HGD, it has been shown that the emplacement of the mineralization was made through hydrothermal fluid events. The chemistry of the hydrothermal fluids led to destruction of magnetite, and results in a reduction of the magnetic field response (Leblanc et al., 2012). Therefore, this type of mineralization is associated to magnetic lows. One other very interesting finding is that the mineralizing hydrothermal fluids also resulted in potassic alteration halos which were successfully mapped with airborne radiometric data acquired in the Williams Mine vicinity (Manning et al., 1998). In particular, the K/Th ratio was proved to correlate very well with gold mineralization.

The data was therefore analysed to identify areas with similarities to the geophysical signature of the HGD in particular, and of other gold occurrences in general.

Magnetic data

The residual TMI data are presented in Figure 8 together with TDEM anomalies. The magnetic data varies over a relatively narrow range of 556 nT.

Two main families of magnetic lineaments are obvious in the area. A first family is generally aligned N-S while a second one is preferentially striking NW-SE. Both families are very likely related to regional intermediate/mafic dykes. A few other isolated magnetic lineaments, generally weaker in intensity and shorter in strike length, are dispersed locally with no clear dominant orientation, and relate to local higher concentration in magnetite/pyrhotite content of rocks.

The background magnetic signal is weaker in the western and southwestern part of the block, which is characteristic of sedimentary rocks. The magnetic background values are stronger elsewhere in the block, and shows increased signal variability, and this is more indicative of intermediate intrusive or volcanic rocks. In the northeastern part of the block, a significant magnetic low region striking NW-SE could be related to a fault structure or deformation zone. This is further supported by the fact that some of the N-S dykes appear

broken up and locally twisted or deformed in this area. As stated above, local areas with weak magnetic signal have possibly been affected by hydrothermal fluids causing magnetite depletion, and therefore this possible deformation corridor should be treated as an area of great exploration potential.

Areas with the strongest magnetic signal are better seen on Figure 9 which shows the residual TMI data with a linear color distribution.

In some areas, the magnetic response is changing abruptly, which denotes major faults crossing the blocks. Shorter wavelength anomalies are greatly enhanced on the First Vertical Derivative (FVD) of the TMI (Figure 10). Since the FVD attenuates longer wavelength anomalies, it is the preferred product for structural interpretation. Structural features can be inferred from cross-cutting of magnetic lineaments, or abrupt change in lineament's wavelength, and also by a joint analysis of topography data (Figure 11). As well, narrow magnetic highs or lows can sometime indicate faults or shear zones enriched or depleted in magnetic minerals. Based on these interpretation techniques, a number of possible faults/shear zones have been interpreted and are shown as thick black dashed lines on all the figures of this section. It should also be kept in mind that some of the magnetic dykes seen in the area may have been emplaced in old faulted zones.

These interpreted structural features should be considered as potential exploration targets if other indication of gold favorable environment is found in their vicinity.

Figure 8: **Residual TMI data with equal area color distribution**

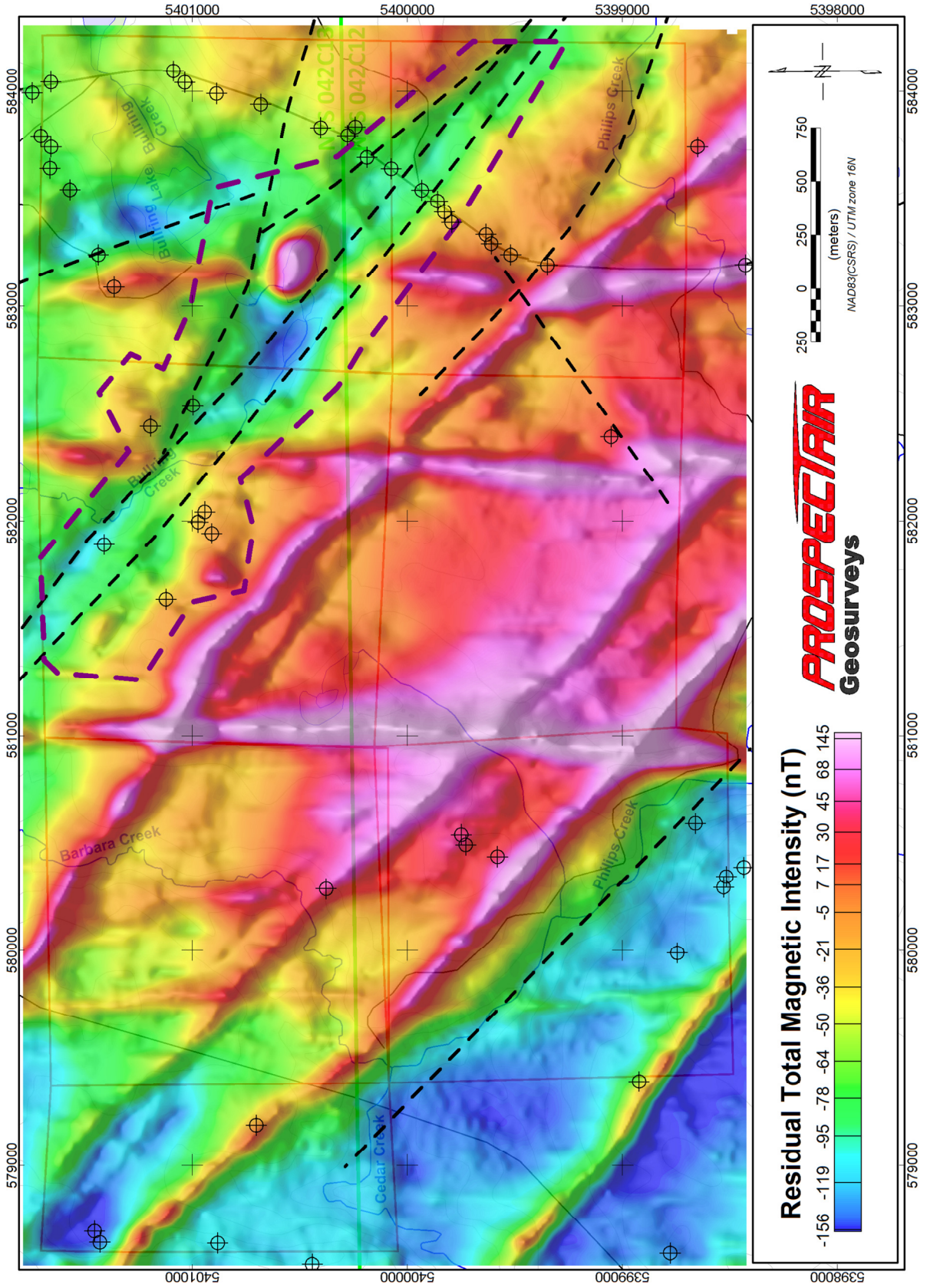

Figure 9: **Residual TMI data with linear color distribution**

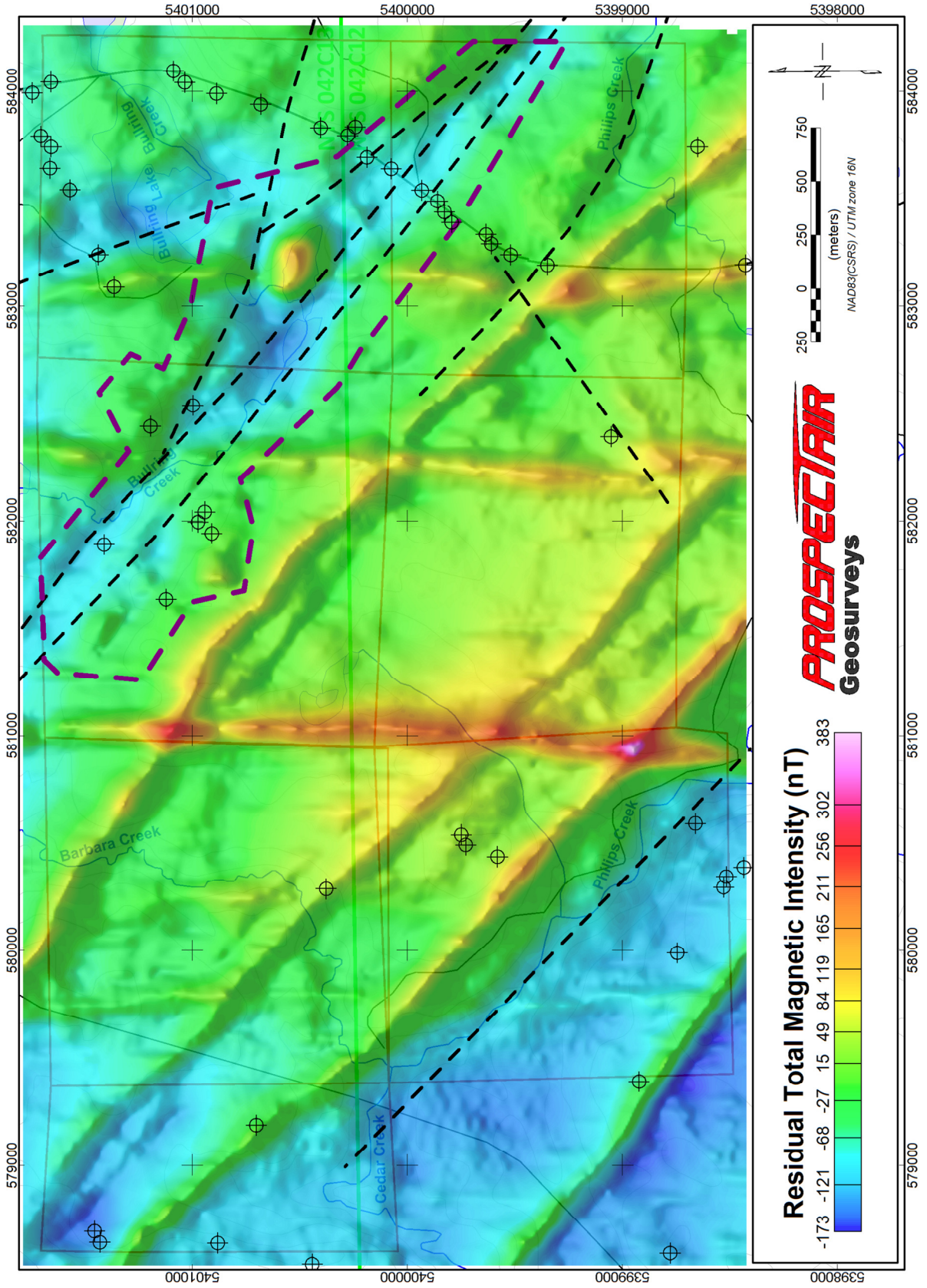

Figure 10: **First Vertical Derivative of TMI**

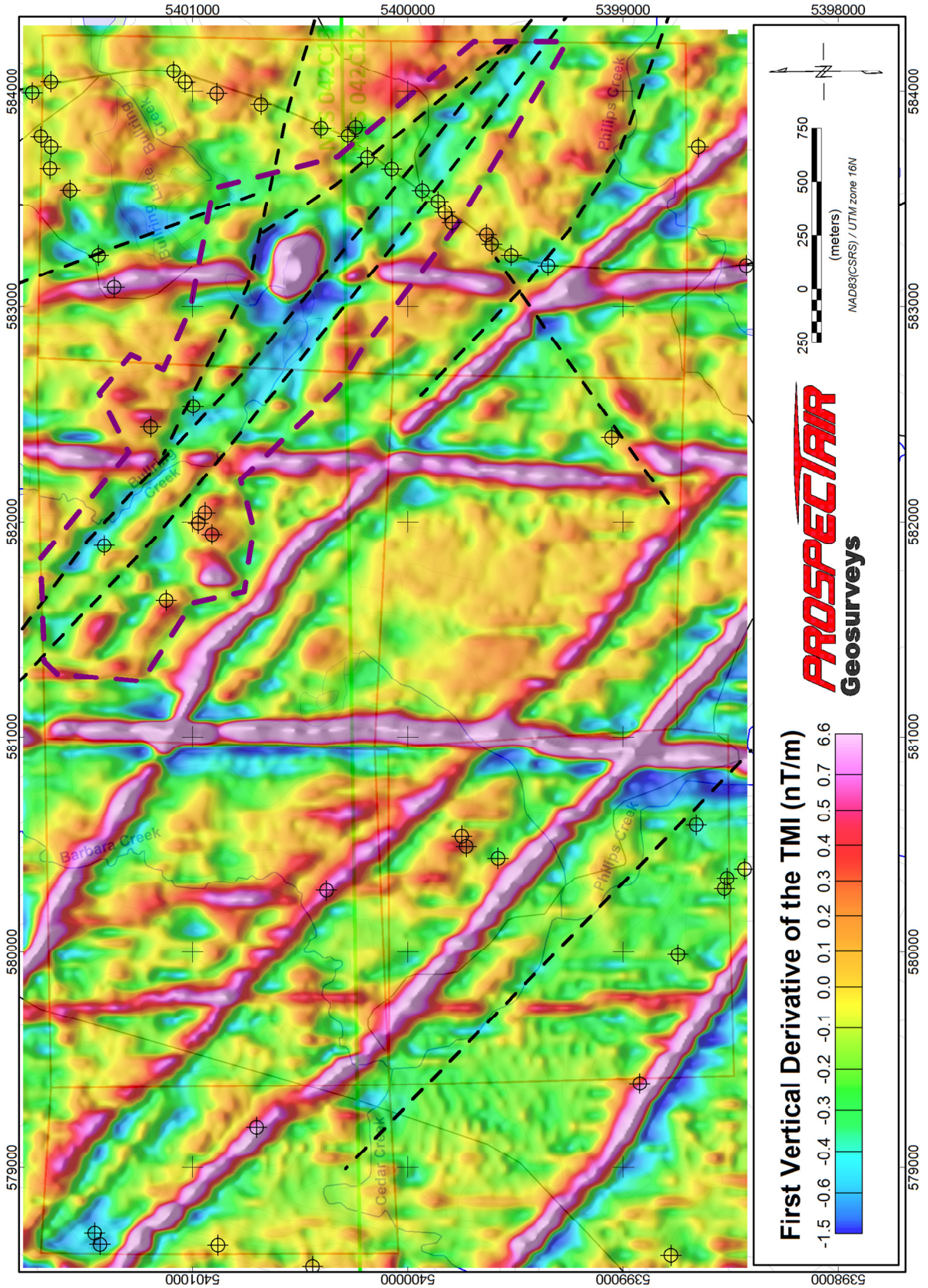

Figure 11: **Digital Elevation Model and interpreted structures**

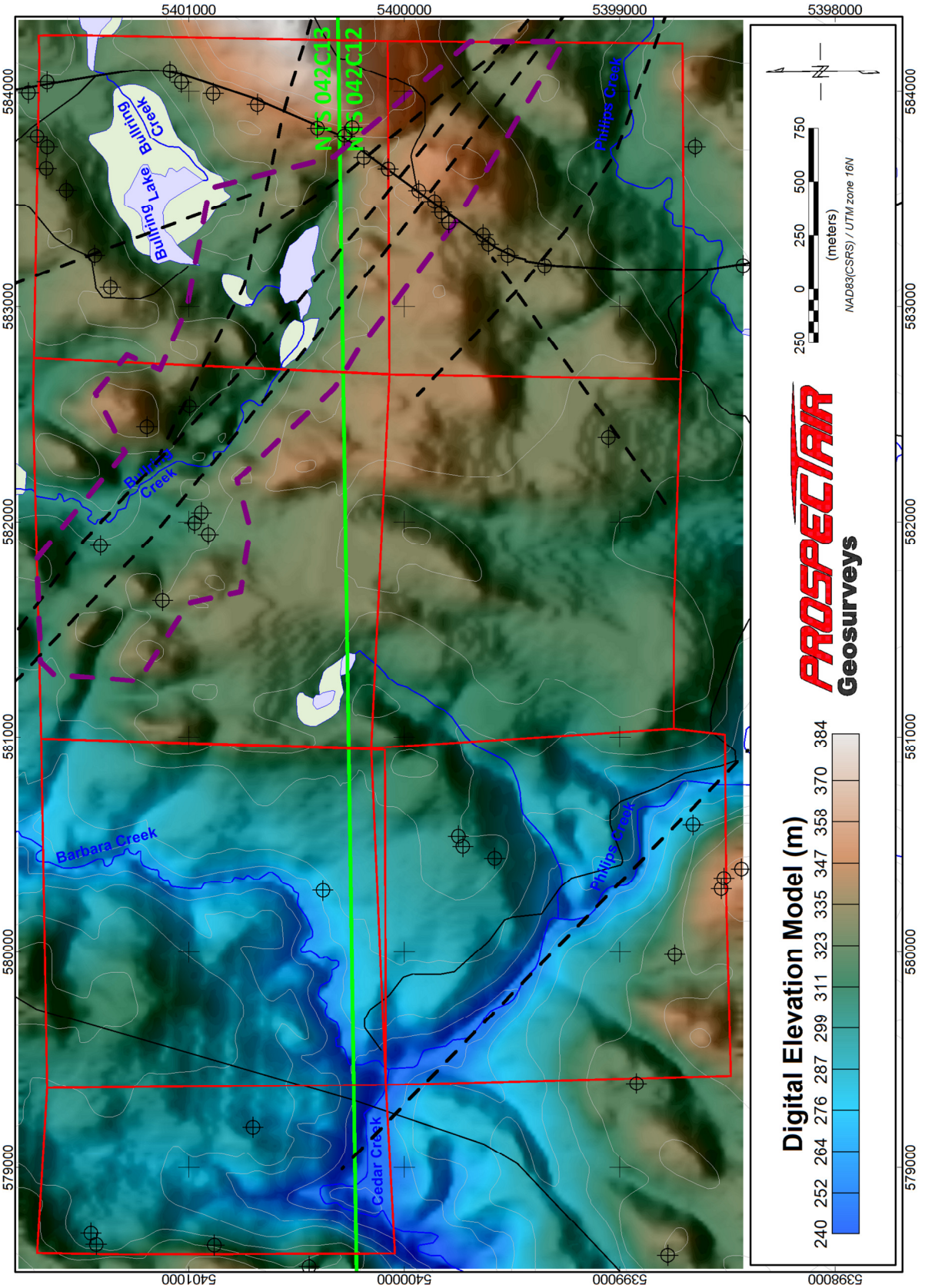

Time-Domain Electromagnetic data

There is no automatic picking program involved in the interpretation procedures of the ProspecTEM system. Identification of the EM anomalies is made from the EM profiles. The location of anomalies is based on the assumption that the causative source is a somewhat thick or flat lying conductor, which would generate an anomaly approximately centered over the conductor (Figure 12, A). It is important to understand that some other conductive body could generate a strong EM response that is offset from the mass centre of the source. For instance, a thin conductor with a steep dip would generate an "M" shape anomaly (Figure 12, B), with the stronger shoulder on the dip side. Therefore, caution must be taken when planning work at the location of an anomaly. It is recommended to combine any other available geoscientific information and to review the EM anomaly location before investigating an anomaly of interest.

Figure 12: **Example of EM response over thin conductors**

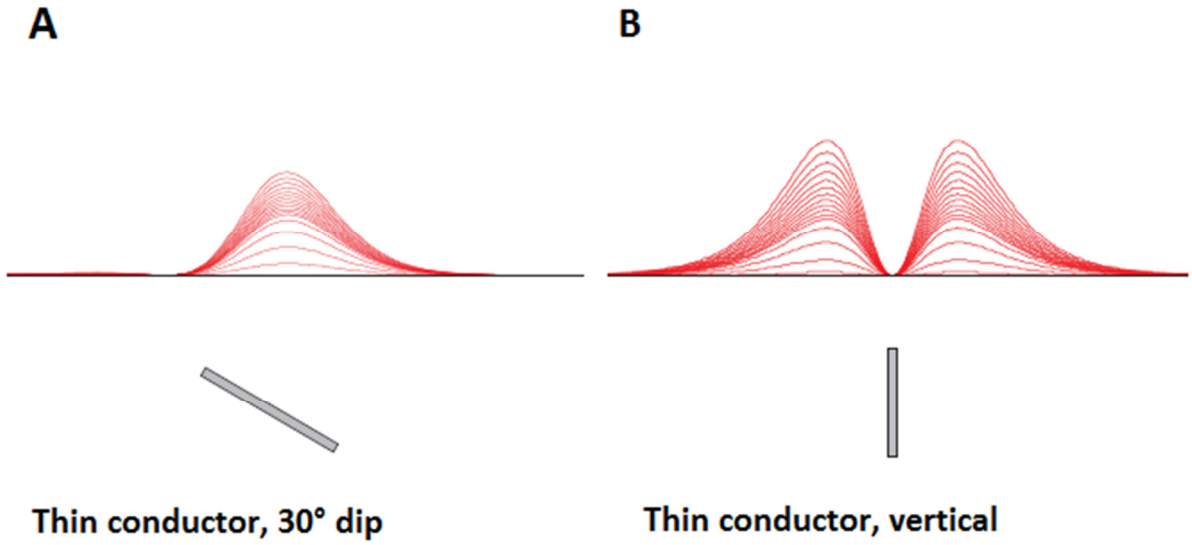

The classification of anomalies is based on the calculated time constant. The EM time constant is a general measure of the speed of decay of the electromagnetic response and reflects the "conductance quality" of a source. The decay rate of the secondary EM field recorded by the TDEM system is a function of the conductivity and geometry of conductors detected. A weak conductor, such as shallow conductive overburden, will show rapid response decay, thus a small value of the time constant (TAU). Conversely, a good conductor, such as a graphite or sulphide orebody, will have a response decaying slowly, relating to a large TAU value. The TAU is calculated using proprietary software and is derived from the best exponential least squares fit for channels Z13 to Z27. Moreover, the resulting exponential best fit of the decay curve is extrapolated to the zero delay time, which can be used to compare the amplitude of anomalies.

On the Hemlo block, 51 EM anomalies are identified, classified and listed (Appendix A). However, all of these anomalies are considered really marginal as they are only slightly exceeding the expected noise envelope of the system. This can be seen on Figure 13 which uses a standard colour bar for the TDEM data from this system. These anomalies are reported on all the figures of this section, and the symbols used are similar to the legend on the maps.

It is important to point that human infrastructure such as power lines are known to create cultural interference and to alter the signal quality and generate anomalies not related to the geology. This is clearly the case for EM anomalies found along the road 614 found to the east of the block. A total of 20 anomalies appear to be related to this road and associated power line.

This leaves 31 marginal anomalies that could be related to conductive overburden or weak bedrock conductors. Some of them are associated to magnetic anomalies, or occur very close to them. In these instances, the good correlation of EM and MAG anomalies suggest that sulphides, including pyrrhotite, are likely to compose at least part of the anomaly sources. Since the HGD does not have any particular EM signature, the lack of strong EM anomalies within the surveyed block should not be seen as an obstacle to gold exploration in the area. Instead, it implies that precedence should be given to the magnetic and spectrometric data for the definition of prospective environments.

Figure 13: **Early Off-Time TDEM response**

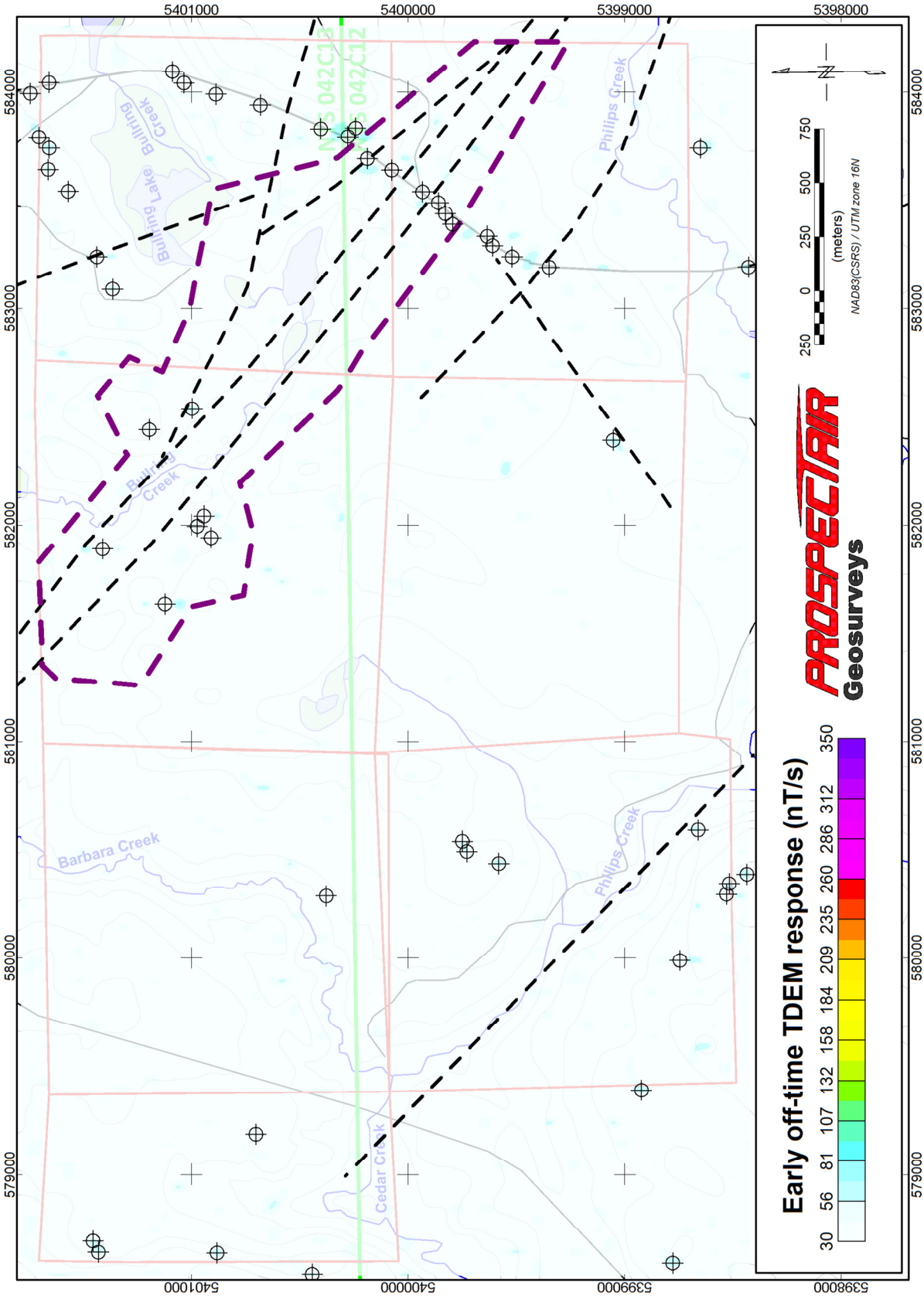

Spectrometric data

Since gamma-rays are quickly absorbed by matter, the response measured by the airborne system only comes from the first few centimeters of the ground. This has implication when interpreting spectrometric results and the radiometric method is therefore treated as a surficial exploration tool, with no penetration.

Water accumulation in topographic lows attenuates most of the signal, and the response is therefore partly controlled by non-geological elements. Nonetheless, it is a very useful method for discriminating different rock types on the basis of their radio-elements content, and can thus be used in support to geological mapping efforts. It is also an effective method at detecting specific rock alteration patterns.

The gamma-ray total count, which sums up gamma-ray counts regardless of their radio-element nature, is the least affected by noise and therefore highlight geological trends particularly well (Figures 14). Areas with strong total count anomalies have some potential to indicate hydrothermal events, since many radio-elements are often concentrated by these events or alteration phenomena related to them.

Since potassium alteration is known to be in direct relation to gold mineralization in the case of the HGD, the potassium concentration data, shown in Figure 15, is considered as an important exploration target definition tool in the context of this project. However, the K/Th ratio is considered an even better tool for this matter, since it tends to attenuate effects unrelated to the geology. This is explained below.

As expected, the radiometric response is generally weaker along topographic depressions. In order to compensate for this undesirable effect the calculated radio-elements ratios are also supplied. In theory, interpretation based on ratios of the three main radio-elements, Potassium (K), equivalent Uranium (U) and equivalent Thorium (Th), has advantages over the use of direct element concentration because natural variations from the level of rock exposition are adjusted for. Variable overburden thickness and extents, vegetation, topography and surface water content strongly control the intensity of gamma-rays response for all three elements. However, since all three elements are affected in the same manner by these variables, the ratios enable mitigation of these effects and enhance response from the geology. Note that in the ratios data maps some areas do not have any data. This is done on purpose when the signal for one of the radio-elements is simply too low to yield a reliable ratio value.

The Th/K ratio data is presented on Figure 16. Note that this data is shown with a reversed color bar, resulting in low Th/K values, equivalent to high K/Th values, to be displayed as warm colors. Areas possibly affected by potassium alteration would therefore appear as purple/red on this image. As already stated, the K/Th ratio was proved to correlate very well with gold mineralization in the Hemlo Gold Deposit context. Consequently, areas with much stronger K/Th values should be prioritized for investigation when other favorable indicators are found in the vicinity.

Figure 14: **Gamma-ray total count**

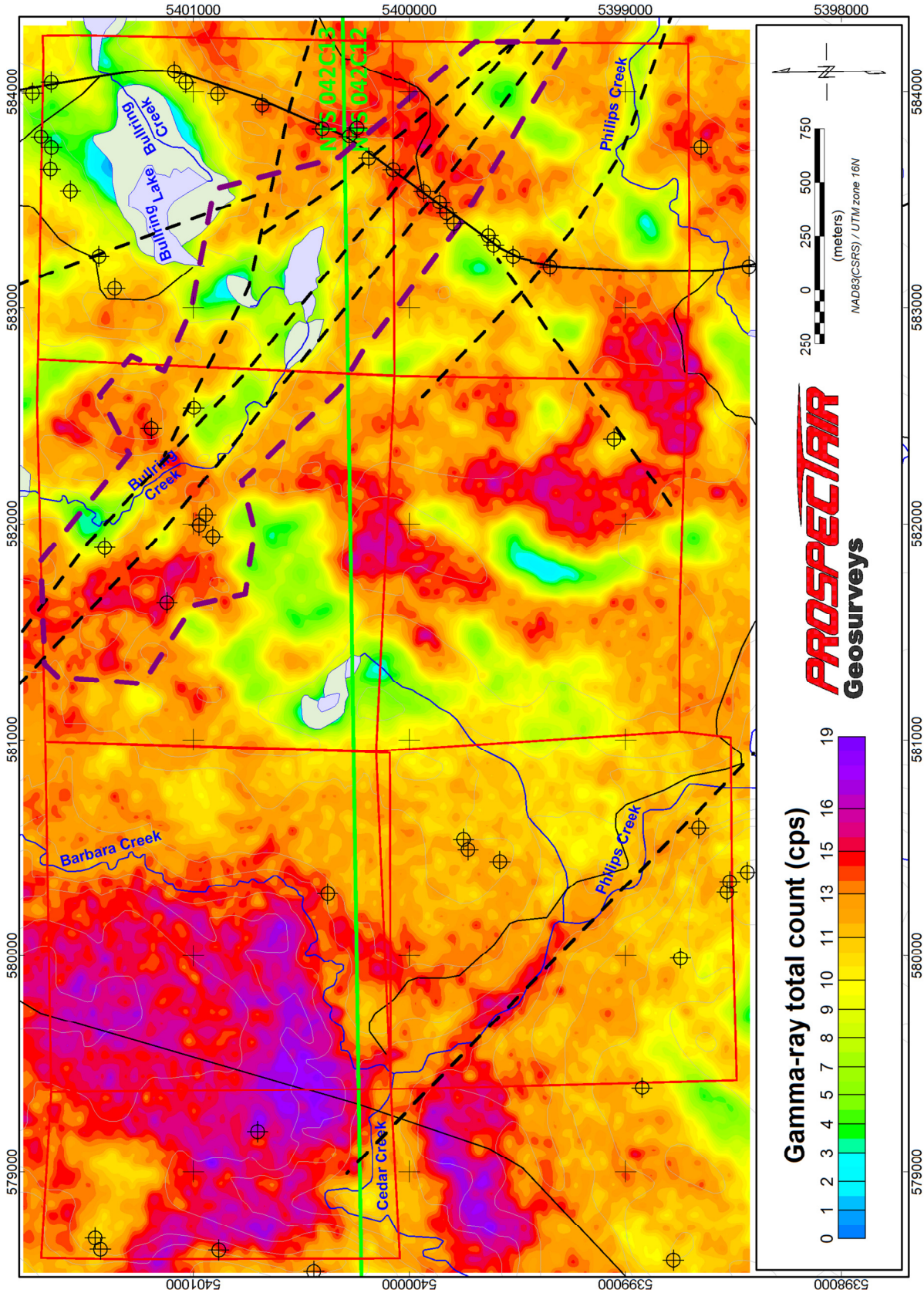

Figure 15: **Potassium concentration**

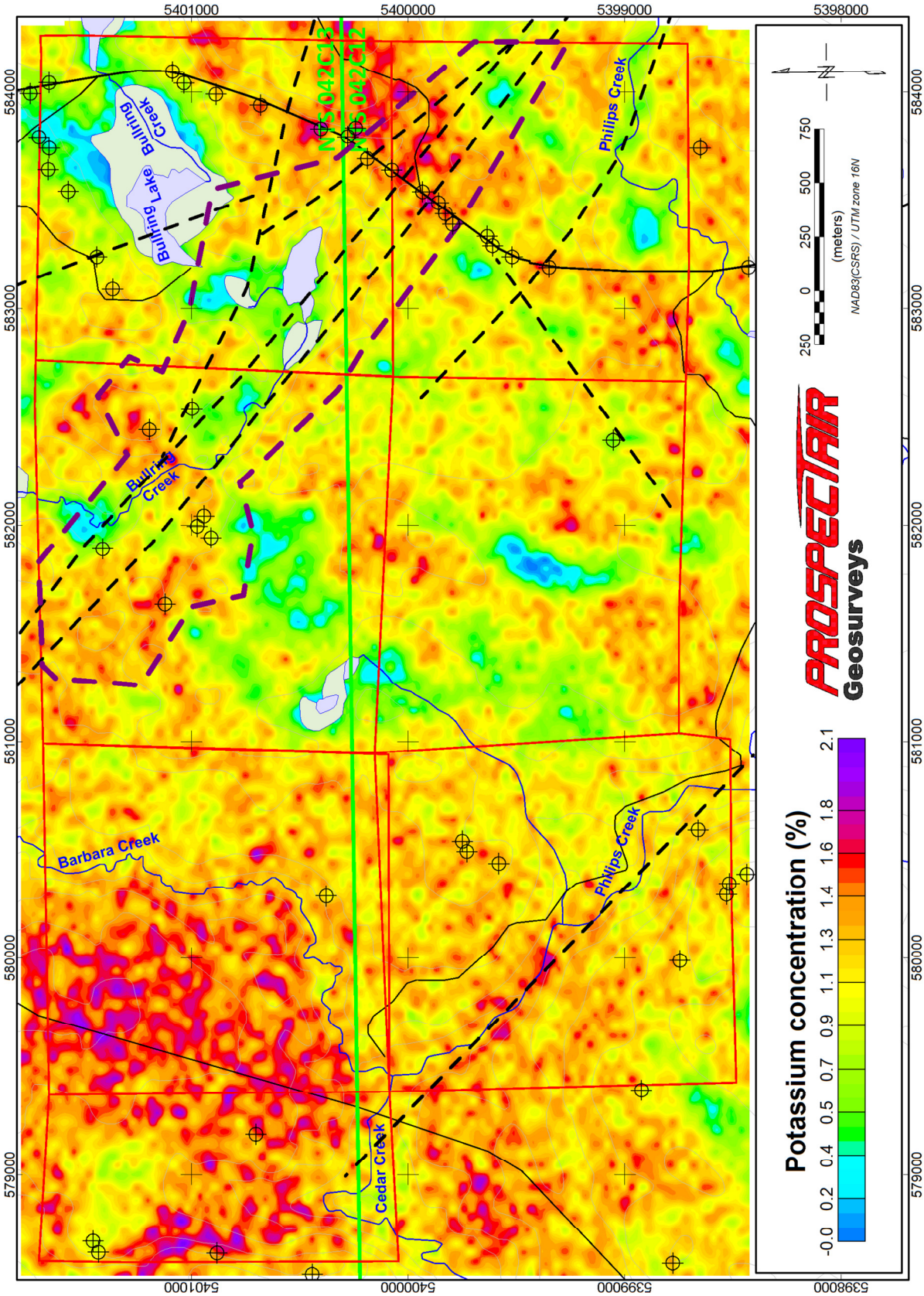

Figure 16: **Thorium/Potassium ratio**

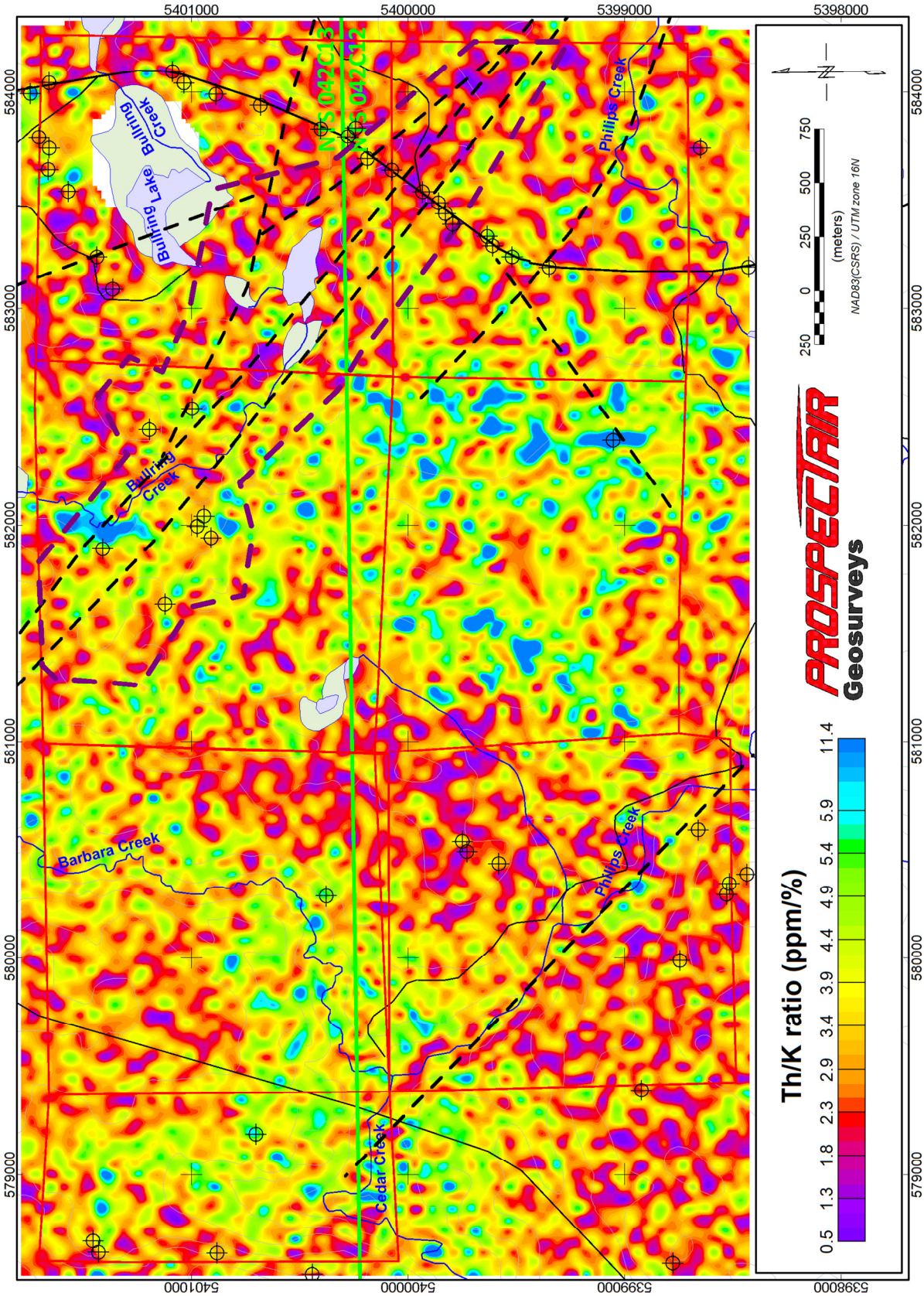

The response found in the block is very variable for the three radio-elements analyzed. The spectrometric ternary image (Figures 17) is especially useful at identifying areas with radio-elements enrichment, and their associations/dissociations. The ternary image shows strong potassium, uranium and thorium concentration in pink, light blue and yellow, respectively. Uranium-thorium, thorium-potassium and potassium-uranium associations appear in green, red and dark blue, respectively. Areas with strong concentration in all elements are shaded and areas with weak concentration are shown in very light colors, almost white in some places. Again, in this exploration context, potassium is known to be a good exploration vector, so areas in pink are of potential interest.

Since overburden thickness may be important in some parts of the surveyed area, the radiometric results possibly mostly reflect the nature of surficial overburden, and thus must be treated the same way as general geochemical data. Glacial dispersion trains must be considered when using the results.

Figure 17: **Spectrometric ternary image**

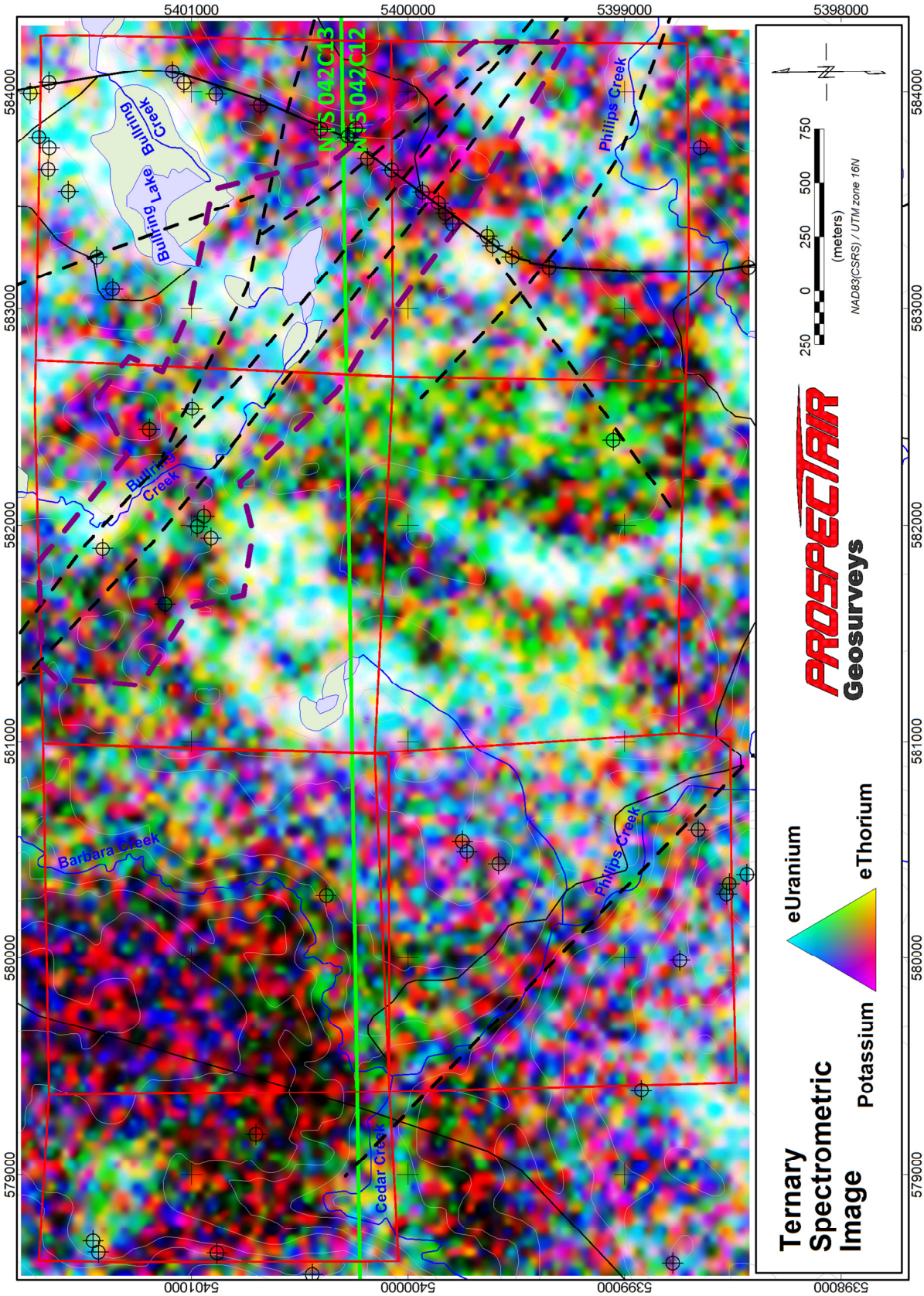

Prospective areas

Several indicators for gold mineralization targeting can be defined based on the geophysical data presented and have been proposed in this report.

For general gold deposits:

- EM anomalies, even weak;
- Weak magnetic high if pyrrhotite/magnetite is associated to gold;
- Structural features interpreted from the magnetic and topographic data.

Specific to the Hemlo Gold Deposit:

- Local magnetic low due to depletion of magnetite by hydrothermal events;
- Potassium anomalies, or high values of the K/Th ratio (low values of Th/K).

Any of these elements taken alone could be sufficient to define an exploration target. However, areas showing combination of some of these indicators should be highly prioritized. Based on this analysis, the most prospective area of the surveyed block has been defined and is shown as thick burgundy dashed lines on the figures found in this section. This proposed prospective area could be updated based on other geoscientific information such as geochemical or geological data.

VIII. WORK RECOMMENDATION

The discussion on the geological implication of the survey data is minimal in this report. A more general study including information regarding the local geology and all other geoscientific data available in the area would be necessary to extract the full potential of the geophysical data.

The prospective area defined in this report should be investigated in priority with basic ground prospection methods. If interesting results are obtained, or if overburden thickness prevents proper ground investigation, it is recommended to use the resistivity/IP technique to conduct exploration and eventually to accurately define drilling targets. This technique has been proven to detect disseminated sulphides associated to gold mineralization for most deposit types, including for the Hemlo Gold Deposit.

IX. FINAL PRODUCTS

Maps

All maps are referred to NAD-83 in the UTM projection Zone 16 North, with coordinates in metres. Maps are at a 1:10,000 scale. Maps are provided in PDF, PNG, Geotiff and Geosoft MAP formats for the products found in Table 13.

Table 13: **Maps delivered**

No.	Name	Description
1	DEM+FlightPath	Digital Elevation Model with flight path
2	TMIcontours	Residual Total Magnetic Intensity contours
3	FVD	First Vertical Derivative of the TMI
4	Total_Count	Gamma-ray total count
5	Potassium	Potassium concentration
6	eUranium	Equivalent Uranium concentration
7	eThorium	Equivalent Thorium concentration
8	Ternary_Spectro	Spectrometric ternary image
9	Ratio_eTh-K	Equivalent Thorium/Potassium ratio
10	Early_Off-Time	Early_Off-Time TDEM response
11	TDEM_Profiles+Anomalies	TDEM profiles with anomalies
12	TMI+TDEM_Anomalies	Residual TMI with TDEM anomalies

Grids

All grids are referred to NAD-83 in the UTM projection Zone 16 North, with coordinates in metres. Grids are provided in Geosoft GRD format, with a 10m grid cell size, for the products listed in Table 14.

Table 14: **Grids delivered**

No.	Name	Description	Units
1	DEM	Digital Elevation Model	m
2	TMI	Total Magnetic Intensity	nT
3	FVD	First Vertical Derivative of TMI	nT/m
4	SVD	Second Vertical Derivative of TMI	nT/m^2
5	TMIres	Residual TMI (IGRF removed)	nT
6	Early_Off-Time	Early Off-Time TDEM response (Channel 13)	nT/s
7	Mid_Off-Time	Mid Off-Time TDEM response (Channel 20)	nT/s
8	Late_Off-Time	Late Off-Time TDEM response (Channel 27)	nT/s
9	TOTcps	Total Count	Cps
10	K	Potassium concentration	%
11	eU	Equivalent Uranium concentration	ppm
12	eTh	Equivalent Thorium concentration	ppm
13	UTHRATIO	Equivalent Uranium/Equivalent Thorium ratio	
14	UKRATIO	Equivalent Uranium/Potassium ratio	
15	THKRATIO	Equivalent Thorium/Potassium ratio	

Digital Line Data

The database is provided at a 0.1 second sampling rate, in Geosoft GDB format, with the channels detailed in Table 15.

Table 15: **MAG-TDEM-SPEC line data channels**

No.	Name	Description	Units
1	UTM_X	UTM Easting, NAD-83, Zone 16N	M
2	UTM_Y	UTM Northing, NAD-83, Zone 16N	M
3	Lat_deg	Latitude in decimal degrees	Deg
4	Long_deg	Longitude in decimal degrees	Deg
5	GPS_Z	Helicopter altitude (w.r.t. MSL)	M
6	Gtm_sec	Second since midnight GMT	Sec
7	Radar	Ground clearance given by the radar altimeter	M
8	DEM	Digital Elevation Model (w.r.t. MSL)	M
9	Mag_Raw	Raw magnetic data	nT
10	Mag_Lag	2.15s lagged magnetic data	nT
11	Gnd_mag	Base station magnetic data	nT
12	Mag_Cor	Magnetic data corrected for diurnal variation	nT
13	TMI	Fully levelled Total Magnetic Intensity	nT
14	TMIres	Residual TMI (IGRF removed)	nT
15	OFF_TIME_Raw	Amplitude of Off-time channels (13 to 36), non-levelled	nT/s
16	OFF_TIME	Amplitude of Off-time channels (13 to 36), fully levelled	nT/s
17	TC_Raw	Raw spectrometric total count	Count/sec
18	K_Raw	Raw count in the Potassium window	Count/sec
19	U_Raw	Raw count in the Uranium window	Count/sec
20	Th_Raw	Raw count in the Thorium window	Count/sec
21	Up_cps	Raw count in the upward Uranium window	Count/sec
22	GRCosmic_cps	Raw count in the Cosmic window	Count/sec
23	TCCORR	Total count corrected	Count/sec
24	KCORR	Potassium concentration at ground level	%
25	UCORR	Equivalent Uranium concentration at ground level	ppm
26	THCORR	Equivalent Thorium concentration at ground level	ppm
27	RALTSTP	Radar clearance at Standard Temperature-Pressure	m
28	GRSPD_cps	Full 256 channels spectrum for downward crystals (1Hz)	Counts/sec
29	GRSPU_cps	Full 256 channels spectrum for upward crystal (1Hz)	Counts/sec

Project Report

The report is submitted in PDF format. The anomaly tables presented in annexes are also provided as separate Excel spreadsheets.

Interpretation Features

The structural features and prospective area interpreted in this report are supplied in the Esri shapefile SHP format.

Respectfully submitted,

_____

Joël Dubé, P. Eng.
August 31st 2016

X. STATEMENT OF QUALIFICATIONS

Joël Dubé
7977 Décarie Drive
Ottawa, ON, Canada, K1C 3K3

Phone: 819.598.8486
E-mail: jdube@ddgeoscience.ca

I, Joël Dubé, P.Eng., do hereby certify that:

1. I am a consultant in geophysics, President of Dynamic Discovery Geoscience Ltd., registered in Canada.

2. I earned a Bachelor of Engineering in Geological Engineering in 1999 from the École Polytechnique de Montréal.

3. I am an Engineer registered with the Ordre des Ingénieurs du Québec, No. 122937, and a Professional Engineer with Professional Engineers Ontario, No. 100194954 (CofA No. 100219617) and with the Association of Professional Engineers and Geoscientists of New Brunswick, No. L5202 (CofA No. F1853).

4. I have practised my profession for 17 years in exploration geophysics.

5. I have not received and do not expect to receive a direct or indirect interest in the properties covered by this report.

Dated this 31st of August, 2016

_____
Joël Dubé, P. Eng. #100194954

XI. REFERENCES

Doyle, H.A., 1990. *Geophysical Exploration for Gold – A Review*; Geophysics, v.55(2); p. 134-146

Hallof, P.G. and Yamashita M., 1984. *The Use of the Induced-Polarization Method to Locate Gold-Bearing Sulfide Mineralization*; SEG Abstracts 1984; p. 304-306

Leblanc, G.E., Lee, M.D. and Morris W.A., 2012. *A simple adaptable data fusion methodology for geophysical exploration*; Exploration Geophysics, v.43(3); p. 190-197

Manning, S.E., Morris W.A. and Leblanc, G.E., 1998. *Multi-Scale Radiometric Mapping of Potassium Alteration: An Example from Hemlo, Ontario;* 68th Annual Internat. Mtg. SEG, Expanded Abstracts, v.98

Pemberton, R.H. and Carriere, D., 1984. *Hemlo Gold Camp Geophysics*; SEG Abstracts 1984; p. 303

XII. Appendix A – Hemlo TDEM anomaly table

Line	UTM_X (m)	UTM_Y (m)	ID	Time Constant (msec)	Amplitude at zero delay (nT/s)
10	578540	5400443	10.01	0.10	0
20	578591	5398779	20.01	0.10	0
30	578637	5400882	30.01	0.10	0
30	578641	5401430	30.02	0.10	0
40	578692	5401454	40.01	0.10	0
140	579186	5400703	140.01	0.10	0
180	579389	5398923	180.01	0.10	0
300	579988	5398746	300.01	0.10	0
360	580293	5398531	360.01	0.10	0
360	580286	5400378	360.02	0.10	0
370	580343	5398518	370.01	0.10	0
380	580387	5398437	380.01	0.10	0
390	580436	5399582	390.01	0.10	0
400	580491	5399729	400.01	0.10	0
410	580537	5399750	410.01	0.10	0
420	580590	5398662	420.01	0.10	0
630	581636	5401122	630.01	0.10	0
680	581889	5401410	680.01	0.10	0
690	581941	5400910	690.01	0.10	0
700	581994	5400973	700.01	0.10	0
710	582041	5400943	710.01	0.10	0
780	582391	5399054	780.01	0.10	0
790	582440	5401195	790.01	0.10	0
810	582537	5400998	810.01	0.10	0
920	583089	5401364	920.01	0.10	0
940	583191	5398429	940.01	0.10	0
940	583190	5399350	940.02	0.10	0
950	583238	5399520	950.01	0.10	0
950	583238	5401437	950.02	0.10	0
960	583289	5399611	960.01	0.10	0
970	583332	5399635	970.01	0.10	0
980	583388	5399795	980.01	0.10	0
990	583437	5399828	990.01	0.10	0
1000	583488	5399861	1000.01	0.10	0
1010	583538	5399933	1010.01	0.10	0
1010	583540	5401569	1010.02	0.10	0
1030	583638	5400075	1030.01	0.10	0
1030	583641	5401661	1030.02	0.10	0
1040	583691	5400188	1040.01	0.10	0
1050	583740	5398652	1050.01	0.10	0
1050	583740	5401657	1050.02	0.10	0
1060	583794	5400278	1060.01	0.10	0
1060	583791	5401704	1060.02	0.10	0
1070	583833	5400243	1070.01	0.10	0
1070	583830	5400403	1070.02	0.10	0
1090	583938	5400682	1090.01	0.10	0
1100	583989	5400888	1100.01	0.10	0
1100	583993	5401744	1100.02	0.10	0

1110	584041	5401035	1110.01	0.10	0
1110	584042	5401657	1110.02	0.10	0
1120	584094	5401088	1120.01	0.10	0